

On the Benefit of Re-optimization in Optimal Control under Perturbations*

Lars Grüne¹ and Vryan Gil Palma¹

Abstract—We consider a finite-horizon optimal control problem for a system subject to perturbations. We compare the performance of the nominal optimal control sequence under perturbations with a shrinking horizon strategy in which a re-optimization for the nominal model is performed in each sampling instant using the current perturbed system state as new initial value. We analyze the potential performance improvement using suitable moduli of continuity as well as stability and controllability properties and illustrate our findings by numerical simulations.

I. INTRODUCTION

Receding horizon control (RHC), also known as model predictive control (MPC) is a control strategy based on the solution, at each sampling instant, of an optimal control problem (OCP) over a chosen horizon. In this optimization-based control technique, an OCP is solved at every sampling instant to determine a sequence of input moves that controls the current and future behavior of a physical system in an optimal manner. Typically for an RHC scheme, after applying the first element of the optimal sequence of input moves, the fixed optimization horizon is shifted by one sampling time into the future and the procedure is repeated, i.e., a re-optimization is performed. In this work, we consider the particular case of an RHC scheme, in which the prediction horizon is decreased by one sampling interval in each re-optimization.

This type of RHC scheme is typically applied to batch processes which are widely seen in various sectors of chemical and manufacturing industries including food products, pharmaceuticals, chemicals products, semiconductors, etc [9]. Batch processes typically refer to the processing of specific quantities of raw materials for a finite duration of time, called a cycle, to form or produce a finite quantity of end product. At the end of a cycle, initial process conditions are reset to run another cycle [7]. Due to the fixed final batch time, the optimal control problem to be solved by RHC is defined on a finite horizon and consequently the prediction horizon of the RHC implementation ‘shrinks’ by one sampling interval in each iteration [9]. This has led to the term ‘shrinking horizon MPC’ [6] with early applications seen in [4], [6], [14].

As a consequence of the dynamic programming principle, in the absence of model uncertainties and disturbances the

*This research is supported by the European Union under the 7th Framework Programme FP7-PEOPLE-2010-ITN, Grant agreement number 264735-SADCO.

¹Lars Grüne lars.gruene@uni-bayreuth.de and Vryan Gil Palma vryan.palma@uni-bayreuth.de are with the Chair of Applied Mathematics, Department of Mathematics, University of Bayreuth, 95440 Bayreuth, Germany

optimal trajectory resulting from the re-optimization with a shrunken horizon coincides with the tail of the optimal trajectory obtained in the previous iteration. Hence, we can only expect a benefit from re-optimization if a perturbation acts on the system. Conceptually, the idea of shrinking horizon MPC has strong similarities to sensitivity-based techniques in order to cope with perturbations [2], [8], [11], in which instead of a full re-optimization only an approximate update of the optimal control based on updated state information is performed. This idea can also be used in moving horizon MPC in order to reduce the number of full optimizations in the context of the so-called real-time optimization [3] or multistep feedback laws [10]. While in this paper we only consider the shrinking horizon setting with full re-optimization, we expect that the results can be extended to sensitivity updates and moving horizon multistep MPC.

Despite the long history of the method, we are not aware of rigorous results which quantify the benefit of the re-optimization in terms of the objective of the optimal control problem in the presence of persisting perturbations. While many papers address feasibility issues — which is an important and serious problem in its own right — results on the performance of the controller and its potential improvement due to re-optimization are to the best of our knowledge missing up to now. This is the gap we intend to close with this paper. More precisely, we compare three different settings: the open-loop controller for the nominal system, the nominal open-loop controller applied to the perturbed system and shrinking horizon RHC, i.e., the controller for which at each time step wherein perturbation is experienced, we perform re-optimization. Our analysis reveals that the potential improvements of re-optimization depend on the moduli of continuity of the optimization objective on the one hand and of the optimal value function on the other hand. For the special case of linear quadratic problems we moreover show how these moduli depend on stability and controllability properties of the system and confirm our theoretical findings by numerical simulations.

The paper is organized as follows. In Section II, we define our setting and give basic tools needed for our analysis such as the dynamic programming principle and uniform continuity of functions. In Section III, we define systems with perturbations and introduce a notation that enables us to keep track of the number of experienced perturbations and performed re-optimizations along a state trajectory. In Section IV and V, we conduct an analysis on the benefits from re-optimization under perturbations by comparing the three settings described above and discussing concepts of

controllability and stability. In Section VI we illustrate our theoretical findings by numerical examples and finally, we give an outlook and conclusion in Section VII.

II. PRELIMINARIES

Consider the nonlinear discrete time control system

$$x(k+1) = f(x(k), u(k)) \quad (1)$$

where x is the state and u is the control value. Let the vector spaces X and U be state and control spaces, respectively. For a given state constraint set \mathbb{X} and control constraint set \mathbb{U} we require $x \in \mathbb{X} \subseteq X$ and $u \in \mathbb{U}(x) \subseteq U$. The notation $x_u(\cdot, x_0)$ (or briefly $x_u(\cdot)$) denotes the state trajectory when the initial state x_0 is driven by control sequence $u(\cdot)$.

We consider the minimization problem

$$\min_{u(\cdot) \in \mathbb{U}^N(x_0)} J_N(x_0, u(\cdot)) \quad \mathcal{P}_N(x_0)$$

for an objective function $J_N(x_0, u(\cdot))$ representing a cost associated with an initial state x_0 at reference time 0, a control sequence $u(\cdot)$ and optimization horizon N . The objective function is given by

$$J_N(x_0, u(\cdot)) := \sum_{k=0}^{N-1} \ell(x_u(k, x_0), u(k))$$

and the minimization is performed over all control sequences $u(\cdot) \in \mathbb{U}^N(x_0)$ with

$$\mathbb{U}^N(x_0) := \left\{ u(\cdot) \in U^N \mid \begin{array}{l} x_u(k+1, x_0) \in \mathbb{X} \text{ and} \\ u(k) \in \mathbb{U}(x_u(k, x_0)) \\ \text{for all } k = 0, \dots, N-1 \end{array} \right\}.$$

The said problem is parametric with respect to the initial value x_0 and for this reason we denote it by $\mathcal{P}_N(x_0)$. Sometimes we also use the notation $\mathcal{P}_N(x_0, k_0)$ in order to emphasize that x_0 is the initial state at initial time k_0 .

We define the optimal value function by

$$V_N(x_0) := \inf_{u(\cdot) \in \mathbb{U}^N(x_0)} J_N(x_0, u(\cdot))$$

and the control sequence $u^*(\cdot) \in \mathbb{U}^N(x_0)$ for which $V_N(x_0) = J_N(x_0, u^*(\cdot))$ is called the optimal control sequence. We note that the optimal control sequence $u^*(\cdot)$ may not exist or may be non-unique.

One important concept that we will be using in our analysis is the dynamic programming principle which relates the optimal value functions of OCPs of different optimization horizon length for different points along a state trajectory [5], [1].

Theorem 1: (Dynamic programming principle) Let x_0 be an initial state value. Let $u^*(0), u^*(1), \dots, u^*(N-1)$ denote an optimal control sequence for $\mathcal{P}_N(x_0)$ and $x_{u^*}(0) = x_0, x_{u^*}(1), \dots, x_{u^*}(N)$ denote the corresponding optimal state trajectory. Then for any i , $i = 0, 1, \dots, N-1$, the control sequence $u^*(i), u^*(i+1), \dots, u^*(N-1)$ is an optimal control sequence for $\mathcal{P}_{N-i}(x_{u^*}(i))$.

Also, to facilitate the discussion for uniform continuity of the involved functions, we consider the following definition.

Definition 2: Consider vector spaces Z and Y , a set $A \subset Z$ and an arbitrary set W

- i. a function $\phi : Z \rightarrow Y$ is said to be uniformly continuous on A if there exists a \mathcal{K} -function¹ ω such that for all $z_1, z_2 \in A$

$$\|\phi(z_1) - \phi(z_2)\| \leq \omega(\|z_1 - z_2\|).$$

- ii. a function $\phi : Z \times W \rightarrow Y$ is said to be uniformly continuous on A uniformly in $v \in W$ if there exists a function $\omega \in \mathcal{K}$ such that for all $z_1, z_2 \in A$ and all $v \in W$

$$\|\phi(z_1, v) - \phi(z_2, v)\| \leq \omega(\|z_1 - z_2\|).$$

The function ω is called the modulus of continuity.

Similar to that found in the appendix of [12], the following theorem gives sufficient conditions for which the optimal value function is a uniformly continuous function without state constraints, i.e., $X = \mathbb{X} = \mathbb{R}^n$.

Theorem 3: (Uniform continuity of $V_N(\cdot)$) Let $\mathbb{X} = \mathbb{R}^n$, $\mathbb{U}(x) \equiv \mathbb{U}$ and suppose that $J_N : \mathbb{R}^n \times \mathbb{U}^N \rightarrow \mathbb{R}$ is uniformly continuous on a set $S \subset \mathbb{R}^n$ uniformly in $u(\cdot) \in \mathbb{U}^N$. Then $V_N(\cdot)$ is uniformly continuous on S .

Proof: From the assumptions, there exists $\omega_{J_N} \in \mathcal{K}$ such that

$$\|J_N(x_1, u(\cdot)) - J_N(x_2, u(\cdot))\| \leq \omega_{J_N}(\|x_1 - x_2\|) \quad (2)$$

for all $x_1, x_2 \in S$ and all $u(\cdot) \in \mathbb{U}^N$. Since (2) holds for any choice of $u(\cdot) \in \mathbb{U}^N$, let $\varepsilon > 0$ and suppose $u_\varepsilon^2(\cdot)$ is an ε -optimal control for $\mathcal{P}_N(x_2)$. This implies

$$\begin{aligned} V_N(x_1) - V_N(x_2) &\leq J_N(x_1, u_\varepsilon^2(\cdot)) - V_N(x_2) \\ &\leq J_N(x_1, u_\varepsilon^2(\cdot)) - J_N(x_2, u_\varepsilon^2(\cdot)) + \varepsilon \\ &\leq \omega_{J_N}(\|x_1 - x_2\|) + \varepsilon. \end{aligned}$$

Likewise, for an ε -optimal control $u_\varepsilon^1(\cdot)$ we have

$$\begin{aligned} V_N(x_2) - V_N(x_1) &\leq J_N(x_2, u_\varepsilon^1(\cdot)) - V_N(x_1) \\ &\leq J_N(x_2, u_\varepsilon^1(\cdot)) - J_N(x_1, u_\varepsilon^1(\cdot)) + \varepsilon \\ &\leq \omega_{J_N}(\|x_2 - x_1\|) + \varepsilon. \end{aligned}$$

Since $\varepsilon > 0$ is arbitrary and this inequality holds for all $x_1, x_2 \in S$, this implies that $V_N(\cdot)$ is uniformly continuous on S . Particularly, for all $x_1, x_2 \in S$

$$\|V_N(x_1) - V_N(x_2)\| \leq \omega_{V_N}(\|x_1 - x_2\|) \quad (3)$$

with $\omega_{V_N} \leq \omega_{J_N}$. ■

In the presence of state constraints, conditions under which a similar result holds become more technical, see, e.g., Proposition 8.40 of [5]. We also note that the modulus ω_{V_N} of continuity represents the sensitivity of the optimal value function to changes in the parameter x of the problem $\mathcal{P}_N(x)$. The proof of the theorem shows that ω_{V_N} is less than or equal to ω_{J_N} , hence we can expect that $\|V_N(x_1) - V_N(x_2)\|$ can not be that much larger than $\|J_N(x_1, u(\cdot)) - J_N(x_2, u(\cdot))\|$ and will typically be smaller. We will further investigate this relation in Section V.

¹A function α is said to be a \mathcal{K} -function if α is continuous and strictly increasing with $\alpha(0) = 0$.

III. PERTURBED SYSTEMS

Using the control system (1) and the optimal control sequence $u^*(0), u^*(1), \dots, u^*(N-1)$ obtained from solving $\mathcal{P}_N(x_0)$, the open-loop controlled system is described by

$$x(k+1) = f(x(k), u^*(k)) \quad k = 0, \dots, N-1 \quad (4)$$

with $x(0) = x_0$ and the corresponding open-loop trajectory denoted by x_{u^*} .

Typically, a real world system is represented by a mathematical model that may fail to take into account disturbance and other various sources of uncertainties. Mathematical models are approximations of real systems, hence a mismatch is inevitable between the predicted states and those that are measured from the real plant. This gives some notion that an open-loop control, the optimal control sequence obtained from the OCP solved at time 0, may not give the best control strategy as the system evolves through time. We aim to investigate the effects of the disturbance and the advantage of using RHC in which we perform re-optimization each time step. In order to simplify the exposition, in the sequel we assume the existence of an optimal control sequence $u^*(\cdot)$ for each $x \in \mathbb{X}$ with $\mathbb{U}^N(x) \neq \emptyset$.

By using shrinking horizon MPC, we can then define a feedback law $\mu : \mathbb{X} \rightarrow \mathbb{U}$ as follows. At each sampling time k , we solve $\mathcal{P}_{N-k}(x(k), k)$, i.e., we perform a re-optimization giving an optimal control sequence $u_k^*(j), j = 0, \dots, N-1-k$ corresponding to the initial value $x_0 = x(k)$ and a resulting trajectory $x_{u_k^*}(j), j = 0, \dots, N-k$. Note that for each sampling time k , the control horizon shrinks. With this, we define

$$\mu(x(k)) = u_k^*(0) \quad k = 0, \dots, N-1$$

and the closed-loop controlled system is described by

$$x(k+1) = f(x(k), \mu(x(k))) \quad k = 0, \dots, N-1 \quad (5)$$

Due to the dynamic programming principle in Theorem 1, in the nominal case where no uncertainties are present, (4) and (5) coincide. But as mentioned above this is not the case in the presence of perturbations. We examine whether RHC addresses the drawbacks that the control design suffers from upon using open-loop control. To this end, we introduce the perturbed closed-loop model

$$x(k+1) = f(x(k), \mu(x(k)) + e(k)) + d(k) \quad (6)$$

where $e(k) \in X$ represents state measurement errors and $d(k) \in X$ represents external perturbation and modeling errors. Due to space limitations, here we only consider $e \equiv 0$ and note that the case $e \not\equiv 0$ can be derived from this case using techniques similar to the treatment in robust stability proofs seen in Chapter 8 of [5].

In order to measure the benefit of re-optimization, i.e., of computing $u_k^*(\cdot)$ in each step, we compare the performance of (6) with that of the perturbed open-loop system given by

$$x(k+1) = f(x(k), u^*(k)) + d(k) \quad (7)$$

To facilitate the discussion on following the trajectories through time where perturbations occur and re-optimization is performed, we use the following notation.

Let $x_{j,p,r}$ denote the state trajectory element at time j that have gone through p perturbations at time instants $t = 1, \dots, p$ where $j \geq p$, and r re-optimizations have been performed at time instants $t = 1, \dots, r$ where $p \geq r$. In this setting, we only put our attention on the nominal and perturbed open-loop trajectories (4) and (7) and on the shrinking horizon MPC trajectory generated by (6) in which a re-optimization is performed in each step. In the newly introduced notation, the trajectories generated by (4), (7) and (6) are given by $x_{j,0,0}$, $x_{j,j,0}$ and $x_{j,j,j}$, respectively, for $j = 0, \dots, N$.

Let $u_{j,p,r}^*$ denote the optimal control sequence obtained by performing a re-optimization with an initial value $x_{j,p,r-1}$ and optimization horizon $N-j$, i.e., $u_{j,p,r}^*$ is obtained by solving $\mathcal{P}_{N-j}(x_{j,p,r-1})$. Since the initial value does not change when performing a re-optimization, the identity $x_{j,p,r-1} = x_{j,p,r}$ holds. We also remark that for our analysis it is sufficient to consider states of the form $x_{j,p,r}$ with $r = 0, p, p-1$.

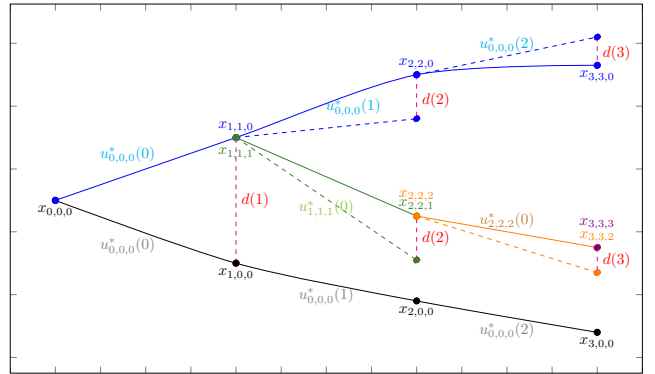


Fig. 1. Trajectories through time where perturbations occur and re-optimizations are performed

Figure 1 illustrates the trajectories through time where perturbations occur and re-optimizations are performed for the final batch time $N = 3$. At time $t = 0$, by solving $\mathcal{P}_3(x_{0,0,0})$, we obtain an open-loop optimal control sequence $u_{0,0,0}^*(j) = u^*(j)$, $j = 0, 1, 2$ for which we can generate a nominal open-loop trajectory $x_{j,0,0}$, $j = 0, \dots, 3$ via (4) shown in black in the sketch. For an additive perturbation $d(\cdot)$, the blue trajectory in Figure 1 indicates the open-loop perturbed trajectory $x_{j,j,0}$, $j = 0, \dots, 3$ generated by (7). Here each transition (shown in solid blue) is composed of the nominal transition $f(x_{j,j,0}, u_{j,0,0}^*(j))$ (blue dashed) followed by the addition of the perturbation $d(j)$ (red dashed). Finally, the trajectory $x_{j,j,j}$ obtained by re-optimization in each step and generated by (6) with perturbation d is shown piecewise in blue, green and orange, with the different colors indicating the different control sequences $u_{j,j,j}^*$, $j = 0, \dots, 2$ whose first pieces are used in the transition. Again, the nominal transition and the effect of the perturbation $d(j)$ are indicated

as dashed lines and the resulting perturbed transitions from $x_{j,j,j}$ to $x_{j+1,j+1,j} = x_{j+1,j+1,j+1}$ as solid lines.

IV. BENEFITS OF RE-OPTIMIZATION

To obtain estimates by comparing trajectories where perturbations may occur and/or re-optimization may be performed, we first introduce some further notation. Similar to how $x_{j,p,r}$ was defined, for $j \geq p$, $p \geq r$, $r = 0, p, p-1$ we define the stage cost

$$\lambda_{j,p,r} = \ell(x_{j,p,r}, u_{r,r,r}^*(j-r)) \quad (8)$$

From this definition, to determine the control needed to compute the stage cost incurred for the state $x_{j,p,r}$ we simply go back to the last instant of the optimization, namely at time r and use the optimal control sequence obtained there wherein horizon $N-r$ and initial value $x_{r,r,r}$ are used.

In order to simplify the numbering in the subsequent computations, we extend the definition to give meaning to the notation when $j < p$, $p \geq r$, $r = 0, p, p-1$ through

$$\lambda_{j,p,r} := \begin{cases} \lambda_{j,j,j} & \text{if } r \neq 0 \\ \lambda_{j,j,0} & \text{if } r = 0. \end{cases} \quad (9)$$

Remark 4: Although the previous discussion yields $x_{j,j,j-1} = x_{j,j,j}$, we see that $\lambda_{j,j,j-1} \neq \lambda_{j,j,j}$ since $\lambda_{j,j,j-1} = \ell(x_{j,j,j-1}, u_{j-1,j-1,j-1}^*(1))$ while $\lambda_{j,j,j} = \ell(x_{j,j,j}, u_{j,j,j}^*(0))$.

In the presence of uncertainties or perturbations, we perform re-optimization in the hope of having a coping mechanism against the differences between the real system and the nominal model to redirect the trajectory back to the desired behavior aiming to stay 'close' to the nominal situation. We investigate whether re-optimization indeed gives such advantage.

The idea is to find quantifiable relations among the various trajectory scenarios. More precisely, we compare the following scenarios.

Definition 5: Given an initial value $x_{0,0,0} = x_0 \in \mathbb{X}$, we define the following performance measures.

- i. The value of the nominal optimal trajectory

$$J_N^{\text{nom}}(x_0) := \sum_{j=0}^{N-1} \lambda_{j,0,0}$$

- ii. The value of the perturbed trajectory with nominal optimal control sequence

$$J_N^{\text{pert}}(x_0) := \sum_{j=0}^{N-1} \lambda_{j,j,0}$$

- iii. The value of the perturbed trajectory with re-optimized control

$$J_N^{\text{reopt}}(x_0) := \sum_{j=0}^{N-1} \lambda_{j,j,j}$$

We recall that in Figure 1 the trajectories corresponding to these performance indices are indicated in, black (i.), blue (ii.) and piecewise in blue, green and orange (iii.) and that they are generated by (4), (7) and (6), respectively. Further, it

is easily seen that $J_N^{\text{nom}}(x_0) = V_N(x_0)$ holds. This nominal optimal value will be our reference in the following analysis.

The following theorem provides the basis for comparing $J_N^{\text{nom}}(x_0)$ and $J_N^{\text{reopt}}(x_0)$. This comparison is then stated in the subsequent corollary.

Theorem 6: Assume $\mathcal{P}_{N-j}(x_{j,j,j})$, $j = 0, \dots, N-1$ is feasible. For $m = 1, \dots, N-1$,

$$\begin{aligned} & \left| V_N(x_{0,0,0}) - \sum_{j=0}^{N-1} \lambda_{j,m,m} \right| \\ & \leq \sum_{j=1}^m |V_{N-j}(x_{j,j-1,j-1}) - V_{N-j}(x_{j,j,j})| \end{aligned} \quad (10)$$

Proof: First, for each time step, we compare the total cost along nominal trajectory to the trajectory where perturbation is introduced in the next time step wherein optimization is performed. Using (8) and (9) we obtain the following set of identities.

$$\begin{aligned} & \left| \sum_{j=0}^{N-1} \lambda_{j,0,0} - \sum_{j=0}^{N-1} \lambda_{j,1,1} \right| \\ & = \left| \lambda_{0,0,0} + \sum_{j=1}^{N-1} \lambda_{j,0,0} - \lambda_{0,1,1} - \sum_{j=1}^{N-1} \lambda_{j,1,1} \right| \\ & = |V_{N-1}(x_{1,0,0}) - V_{N-1}(x_{1,1,1})| \end{aligned}$$

$$\begin{aligned} & \left| \sum_{j=0}^{N-1} \lambda_{j,1,1} - \sum_{j=0}^{N-1} \lambda_{j,2,2} \right| \\ & = \left| \lambda_{0,1,1} + \lambda_{1,1,1} + \sum_{j=2}^{N-1} \lambda_{j,1,1} \right. \\ & \quad \left. - \lambda_{0,2,2} - \lambda_{1,2,2} - \sum_{j=2}^{N-1} \lambda_{j,2,2} \right| \\ & = |V_{N-2}(x_{2,1,1}) - V_{N-2}(x_{2,2,2})| \end{aligned}$$

Inductively, for $m = 1, \dots, N-1$,

$$\begin{aligned} & \left| \sum_{j=0}^{N-1} \lambda_{j,m-1,m-1} - \sum_{j=0}^{N-1} \lambda_{j,m,m} \right| \\ & = \left| \lambda_{0,m-1,m-1} + \dots + \lambda_{m-1,m-1,m-1} \right. \\ & \quad \left. + \sum_{j=m}^{N-1} \lambda_{j,m-1,m-1} - \lambda_{0,m,m} - \dots - \lambda_{m-1,m,m} \right. \\ & \quad \left. - \sum_{j=m}^{N-1} \lambda_{j,m,m} \right| \\ & = |V_{N-m}(x_{m,m-1,m-1}) - V_{N-m}(x_{m,m,m})| \end{aligned}$$

Now with the aid of the identities above, we have the following estimate. For $m = 1, \dots, N-1$,

$$\begin{aligned}
& \left| \sum_{j=0}^{N-1} \lambda_{j,0,0} - \sum_{j=0}^{N-1} \lambda_{j,m,m} \right| \\
&= \left| \sum_{j=0}^{N-1} \lambda_{j,0,0} - \sum_{j=0}^{N-1} \lambda_{j,1,1} + \sum_{j=0}^{N-1} \lambda_{j,1,1} - \dots \right. \\
&\quad \left. \dots + \sum_{j=0}^{N-1} \lambda_{j,m-1,m-1} - \sum_{j=0}^{N-1} \lambda_{j,m,m} \right| \\
&\leq \left| \sum_{j=0}^{N-1} \lambda_{j,0,0} - \sum_{j=0}^{N-1} \lambda_{j,1,1} \right| + \\
&\quad \dots + \left| \sum_{j=0}^{N-1} \lambda_{j,m-1,m-1} - \sum_{j=0}^{N-1} \lambda_{j,m,m} \right| \\
&= |V_{N-1}(x_{1,0,0}) - V_{N-1}(x_{1,1,1})| \\
&\quad + |V_{N-2}(x_{2,1,1}) - V_{N-2}(x_{2,2,2})| + \\
&\quad \dots + |V_{N-m}(x_{m,m-1,m-1}) - V_{N-m}(x_{m,m,m})| \\
&= \sum_{j=1}^m |V_{N-j}(x_{j,j-1,j-1}) - V_{N-j}(x_{j,j,j})|
\end{aligned}$$

$$\begin{aligned}
& \left| \sum_{j=0}^{N-1} \lambda_{j,0,0} - \sum_{j=0}^{N-1} \lambda_{j,1,0} \right| \\
&= \left| \lambda_{0,0,0} + \sum_{j=1}^{N-1} \lambda_{j,0,0} - \lambda_{0,1,0} - \sum_{j=1}^{N-1} \lambda_{j,1,0} \right| \\
&= |J_{N-1}(x_{1,0,0}, u^*(\cdot+1)) - J_{N-1}(x_{1,1,0}, u^*(\cdot+1))| \\
&\text{and} \\
& \left| \sum_{j=0}^{N-1} \lambda_{j,1,0} - \sum_{j=0}^{N-1} \lambda_{j,2,0} \right| \\
&= \left| \lambda_{0,1,0} + \lambda_{1,1,0} + \sum_{j=2}^{N-1} \lambda_{j,1,0} \right. \\
&\quad \left. - \lambda_{0,2,0} - \lambda_{1,2,0} - \sum_{j=2}^{N-1} \lambda_{j,2,0} \right| \\
&= |J_{N-2}(x_{2,1,0}, u^*(\cdot+2)) - J_{N-2}(x_{2,2,0}, u^*(\cdot+2))|
\end{aligned}$$

Inductively, for $m = 1, \dots, N-1$,

$$\begin{aligned}
& \left| \sum_{j=0}^{N-1} \lambda_{j,m-1,0} - \sum_{j=0}^{N-1} \lambda_{j,m,0} \right| \\
&= \left| \lambda_{0,m-1,0} + \dots + \lambda_{m-1,m-1,0} \right. \\
&\quad \left. + \sum_{j=m}^{N-1} \lambda_{j,m-1,0} - \lambda_{0,m,0} - \dots - \lambda_{m-1,m,0} \right. \\
&\quad \left. - \sum_{j=m}^{N-1} \lambda_{j,m,0} \right| \\
&= |J_{N-m}(x_{m,m-1,0}, u^*(\cdot+m)) \\
&\quad - J_{N-m}(x_{m,m,0}, u^*(\cdot+m))|
\end{aligned}$$

With these above, for $m = 1, \dots, N-1$,

$$\begin{aligned}
& \left| \sum_{j=0}^{N-1} \lambda_{j,0,0} - \sum_{j=0}^{N-1} \lambda_{j,m,0} \right| \\
&= \left| \sum_{j=0}^{N-1} \lambda_{j,0,0} - \sum_{j=0}^{N-1} \lambda_{j,1,0} + \sum_{j=0}^{N-1} \lambda_{j,1,0} - \dots \right. \\
&\quad \left. \dots + \sum_{j=0}^{N-1} \lambda_{j,m-1,0} - \sum_{j=0}^{N-1} \lambda_{j,m,0} \right| \\
&\leq \left| \sum_{j=0}^{N-1} \lambda_{j,0,0} - \sum_{j=0}^{N-1} \lambda_{j,1,0} \right| + \\
&\quad \dots + \left| \sum_{j=0}^{N-1} \lambda_{j,m-1,0} - \sum_{j=0}^{N-1} \lambda_{j,m,0} \right| \\
&= \sum_{j=1}^m |J_{N-j}(x_{j,j-1,0}, u^*(\cdot+j)) \\
&\quad - J_{N-j}(x_{j,j,0}, u^*(\cdot+j))|
\end{aligned}$$

Using uniform continuity assumptions on the optimal value function we arrive at the following corollary.

Corollary 7: Suppose V_i , $i = 1, \dots, N$, is uniformly continuous on \mathbb{X} with modulus of continuity ω_{V_i} . Consider an initial value $x_0 \in \mathbb{X}$ and a perturbation sequence $d(\cdot)$ such that $\mathcal{P}_{N-j}(x_{j,j,j})$, $j = 0, \dots, N-1$ is feasible. Then

$$|J_N^{\text{nom}}(x_0) - J_N^{\text{reopt}}(x_0)| \leq \sum_{j=1}^{N-1} \omega_{V_{N-j}}(\|d(j)\|). \quad (11)$$

Proof: The statement follows immediately from Theorem 6 applied with $m = N-1$ observing that $J_N^{\text{nom}} = V_N$ and $x_{j,j,j} - x_{j,j-1,j-1} = d(j)$. \blacksquare

Next we provide the analogous analysis for comparing $J_N^{\text{nom}}(x_0)$ and $J_N^{\text{pert}}(x_0)$.

Theorem 8: Assume $x_{j,j,0} \in \mathbb{X}$ for all $j = 0, \dots, N-1$. For $m = 1, \dots, N-1$,

$$\begin{aligned}
& \left| V_N(x_{0,0,0}) - \sum_{j=0}^{N-1} \lambda_{j,m,0} \right| \\
&\leq \sum_{j=1}^m |J_{N-j}(x_{j,j-1,0}, u^*(\cdot+j)) \\
&\quad - J_{N-j}(x_{j,j,0}, u^*(\cdot+j))| \quad (12)
\end{aligned}$$

Proof: Let $u^* = u_{0,0,0}^*$. Similar to the proof of Theorem 6, we obtain the inequalities

Using uniform continuity assumptions on the objective, the following statement directly follows.

Corollary 9: Suppose J_i , $i = 1, \dots, N$, is uniformly continuous uniformly in u on \mathbb{X} with modulus of continuity ω_{J_i} . Consider an initial value $x_0 \in \mathbb{X}$ and a perturbation sequence $d(\cdot)$ such that $x_{j,j,0} \in \mathbb{X}$ for all $j = 0, \dots, N-1$. Then

$$|J_N^{\text{nom}}(x_0) - J_N^{\text{pert}}(x_0)| \leq \sum_{j=1}^{N-1} \omega_{J_{N-j}}(\|d(j)\|). \quad (13)$$

Proof: The statement follows from Theorem 8 applied with $m = N-1$ observing that $J_N^{\text{nom}} = V_N$ and $x_{j,j,0} - x_{j,j-1,0} = d(j)$. ■

Our analysis reveals that the difference between re-optimizing and not re-optimizing can be quantitatively expressed by the difference between the moduli of continuity ω_{V_i} of the optimal value functions compared to the moduli of continuity ω_{J_i} of the open loop functionals J_i . Indeed, while the difference between J_N^{nom} and J_N^{reopt} is determined by the ω_{V_i} , the difference between J_N^{nom} and J_N^{pert} depends on the ω_{J_i} . In Theorem 3 we have already seen that $\omega_{V_i} \leq \omega_{J_i}$ holds, which implies that re-optimization should not worsen the performance — modulo the conservatism introduced in our analysis due to the triangle inequalities used in the proofs of Theorems 6 and 8.

In practice, our hope is, of course, that re-optimization will not only “not worsen” the performance but rather improve it. For this reason, in the following section, we analyse the moduli of continuity for linear quadratic problems in order to identify situations in which an improvement due to re-optimization can indeed be expected.

V. CONTROLLABILITY AND STABILITY

In this section we consider linear finite dimensional systems of the form

$$x(k+1) = Ax(k) + Bu(k)$$

with $X = \mathbb{X} = \mathbb{R}^n$, $U = \mathbb{U} = \mathbb{R}^m$ and matrices $A \in \mathbb{R}^{n \times n}$, $B \in \mathbb{R}^{n \times m}$. The stage cost is given by the quadratic function

$$\ell(x, u) = x^T Qx + u^T Ru$$

with symmetric and positive definite matrices $Q \in \mathbb{R}^{n \times n}$ and $R \in \mathbb{R}^{m \times m}$.

The simplifying assumptions of linear dynamics, positive definite quadratic costs and no constraints are mainly imposed in order to simplify the presentation of the two key properties controllability and stability in this section. Similar results can also be obtained for nonlinear and constrained problems at the expense of more technically involved definitions and proofs.

We first estimate the modulus of continuity ω_{J_N} .

Proposition 10: Let σ be the eigenvalue of A with maximal modulus $|\sigma|$. Let $S \subset \mathbb{R}^n$ be a bounded set, $N \in \mathbb{N}$

and $\varepsilon > 0$. For a constant $K > 0$ consider the set of control sequences

$$\mathbb{U}_K^N = \{u(\cdot) \in \mathbb{U}^N \mid \|u(k)\| \leq K \text{ for all } k = 0, \dots, N-1\}. \quad (14)$$

Then there exists real constants $c_1 > 0$ and $c_2 = c_2(\varepsilon) > 0$ such that the modulus of continuity ω_{J_N} of J_N on S , uniform in $u(\cdot) \in \mathbb{U}_K^N$ satisfies

$$c_1 r^2 \sum_{k=0}^{N-1} |\sigma|^{2k} \leq \omega_{J_N}(r) \leq c_2 \sum_{k=0}^{N-1} |\sigma|^k r.$$

Proof: For any two initial values $x_1, x_2 \in \mathbb{R}^n$ and any control sequence $u(\cdot) \in \mathbb{U}^N$, the difference $e(k) := x_u(k, x_2) - x_u(k, x_1)$ can be written as

$$e(k) = A^k e(0).$$

Setting $x_1 := 0$ and $x_2 := rv$ where v is an eigenvector for σ with $\|v\| = 1$ then yields $e(0) = rv$ and thus $e(k) = \sigma^k rv$. Since Q is positive definite there exists $c_1 > 0$ with $v^T Q v = c_1$ and for $u(\cdot) := 0$ we obtain

$$\begin{aligned} \ell(x_u(k, x_2), u(k)) - \ell(x_u(k, x_1), u(k)) &= e(k)^T Q e(k) \\ &= c_1 r^2 (\sigma^k)^2. \end{aligned}$$

This yields the lower bound. The upper bound follows on the one hand from the fact that for $\varepsilon > 0$ there exists $\tilde{c}_2 > 0$ such that $\|A^k x\| \leq \tilde{c}_2(|\sigma| + \varepsilon)^k \|x\|$ holds (this follows, e.g., from [13, Satz 11.6]). On the other hand, there exists a compact set $D \subset \mathbb{R}^n$ such that for all $x_0 \in S$ and all $u(\cdot) \in \mathbb{U}_K^N$ the relation $x_u(k, x_0) \in D$ holds for all $k = 0, \dots, N-1$. On this set D the stage cost ℓ is Lipschitz in x with a constant $L > 0$, which yields the claimed upper bound with $c_2 = L \tilde{c}_2$. ■

Observe that the lower bound on $\omega_{J_N}(r)$ is independent of the choice of S , ε , K and N while the upper bound typically depends on these parameters.

Proposition 10 states that the modulus of continuity ω_{J_N} is large whenever $|\sigma|$ is large and small if $|\sigma|$ is small. In particular, ω_{J_N} grows unboundedly in N if the system is not open-loop asymptotically stable, i.e., if $|\sigma| \geq 1$.

Observe that Theorem 3 applies to the setting in this section, hence the upper bound on ω_{J_N} from Proposition 10 also applies to ω_{V_N} . In addition, under suitable conditions, ω_{V_N} can be considerably smaller than ω_{J_N} , as the following proposition shows.

Proposition 11: Assume that the pair (A, B) is controllable. Let $S \subset \mathbb{R}^n$ be a bounded set. Then there exists a real constant $c > 0$ such that the modulus of continuity ω_{V_N} on S satisfies

$$\omega_{V_N}(r) \leq cr$$

for all $N \in \mathbb{N}$.

Proof: Controllability implies that there exists a constant $\tilde{c} > 0$ such that for any $x_0 \in \mathbb{R}^n$ we can find a control $u_{x_0}(\cdot) \in \mathbb{U}^n$ with $\|u_{x_0}(k)\| \leq \tilde{c}\|x_0\|$ for all $k = 0, \dots, n-1$ and $x_{u_{x_0}}(n, x_0) = 0$. This implies that on the bounded set S there exists a uniform upper bound M of V_N which can

be chosen independent of N . Then, positive definiteness of Q and R implies that the optimal trajectories remain in a compact set D and that the optimal control sequences lie in the set \mathbb{U}_K^N from (14), where D and K can also be chosen independent of N .

Now for $N \leq n$ the assertion follows from Proposition 11 in conjunction with Theorem 3. For $N > n$, consider two initial values $x_1, x_2 \in S$ and let $u^*(\cdot)$ be the optimal control for x_1 .

Let $x_0 := x_2 - x_1$ and pick the control sequence $u_{x_0} \in \mathbb{U}^n$ from the controllability property, which we extend with $u_{x_0}(k) := 0$ for all $k \geq n$, implying $x_{u_{x_0}}(k, x_2 - x_1) = 0$ for all $k \geq n$. Then, for $\tilde{u}^* = u^* + u_{x_0}$ we get

$$x_{\tilde{u}^*}(k, x_2) = x_{u^*}(k, x_1) + x_{u_{x_0}}(k, x_2 - x_1) = x_{u^*}(k, x_1)$$

for all $k \geq n$. Since ℓ is Lipschitz on $S \times \mathbb{U}_K$, we can find $\hat{c} > 0$ such that

$$\ell(x_{\tilde{u}^*}(k, x_2), \tilde{u}^*(k)) - \ell(x_{u^*}(k, x_1), u^*(k)) \leq \hat{c} \|x_2 - x_1\|$$

for all $k = 0, \dots, n-1$, while for $k \geq n$ this difference equals 0. This implies the desired estimate with $c = n\hat{c}$. ■

As a consequence, we expect the difference between ω_{J_N} and ω_{V_N} to be particularly large when the system is open-loop unstable (implying a large ω_{J_N}) and controllable (implying a small ω_{V_N}). In the next section, we present examples which numerically illustrate that this is exactly what happens.

VI. NUMERICAL EXAMPLES

Here we consider an illustrative numerical example for which we compare the nominal case J_N^{nom} , the case when nominal solution is applied to perturbed systems J_N^{pert} and the shrinking horizon MPC J_N^{reopt} where the re-optimization is carried out each time step due to the mentioned perturbation. Consider the nominal system described by

$$x^+ = \alpha x + u \quad (15)$$

and the corresponding perturbed system

$$x^+ = \alpha x + u + d \quad (16)$$

where d is an additive perturbation with a performance index $\mathcal{P}_N(x_0)$ wherein

$$\ell(x, u) = x^2 + u^2.$$

Note that the stage cost ℓ forces the optimal trajectory to converge to the origin 0, hence the distance of the perturbed trajectory from the origin can be used as a visual performance measure.

If $|\alpha| < 1$, then (15) is asymptotically stable with 0 as the equilibrium, and for $|\alpha| > 1$, it is unstable. In both cases, the system is controllable. Taking final batch time as $N = 7$, Figure 2 provides a visualization of the trajectories throughout time for a chosen α for $x_0 = -4$. With $i = 0, \dots, N$, $x_{i,0,0}$ represents the nominal trajectory related to $J_N^{\text{nom}}(x_0)$, while $x_{i,i,0}$ denotes the trajectory corresponding to $J_N^{\text{pert}}(x_0)$, i.e., when the nominal open-loop control is applied

to the perturbed system (16). Finally, $x_{i,i,i}$ represents the trajectory with re-optimization, corresponding to $J_N^{\text{reopt}}(x_0)$. The perturbations $d(\cdot)$ are randomly generated from the interval $[-0.1, 0.1]$. Figure 2(top) illustrates the case when $\alpha = 0.5$ for which (15) is stable where the three described trajectories can be compared. Since the system is open-loop stable, one would expect not much improvement from re-optimization, which is exactly what is visible in the figure, as the deviation from the nominal solution is only mildly improved by re-optimization. In contrast to this, Figure 2(bottom) shows the case $\alpha = 1.5$, in which the system is open-loop unstable and controllable. Here our analysis predicts a large benefit of the re-optimization procedure which is clearly visible in the simulation. The similar effect is visible in Table I in which the values of $J_N^{\text{nom}}(x_0)$, $J_N^{\text{pert}}(x_0)$ and $J_N^{\text{reopt}}(x_0)$ for $x_0 = -4$ are shown. In the open-loop unstable and controllable system with $\alpha = 1.5$, one can notice a better performing $J_N^{\text{reopt}}(x_0)$ compared to $J_N^{\text{nom}}(x_0)$. This is due to the fact that here the introduced random perturbations do by chance have a positive effect on the performance because they drive the system faster towards 0.

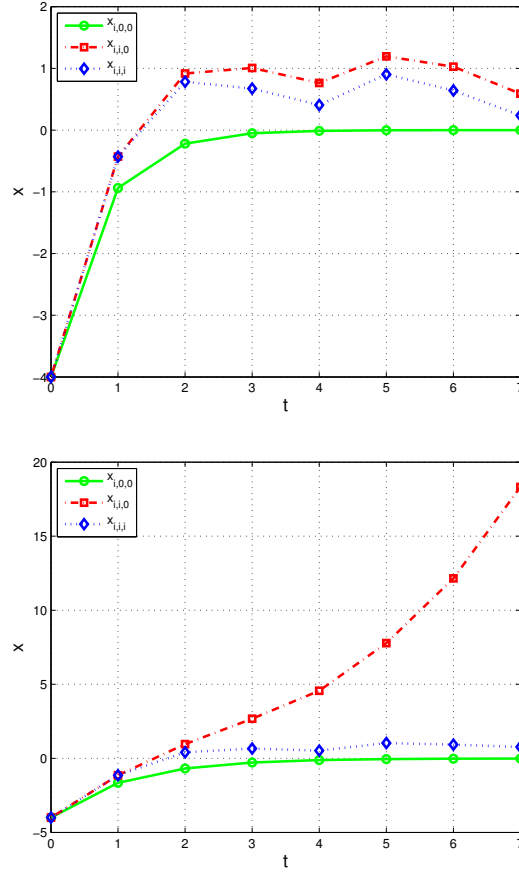


Fig. 2. State trajectories for the stable system with $\alpha = 0.5$ (top) and for the unstable system with $\alpha = 1.5$ (bottom)

Figure 3 and Table II illustrate a case when re-optimization does not give much benefit because the system is not control-

TABLE I
COMPARISON OF CONTROL SCHEME PERFORMANCE

	$\alpha = 0.5$	$\alpha = 1.5$
$J_N^{\text{nom}}(x_0)$	18.1245	42.0829
$J_N^{\text{pert}}(x_0)$	22.6457	613.1214
$J_N^{\text{reopt}}(x_0)$	18.8812	24.8458

lable. In this example, we set $\alpha = 1.5$ and impose a control constraint $u \geq 0$ which renders the system uncontrollable. Figure 3 shows the system behavior for the unstable case $\alpha = 1.5$. Compared to Figure 2(bottom) one sees that the performance of the re-optimization significantly deteriorates, though it still provides some improvement over using the open-loop optimal trajectory. The numerical values in Table II confirm this behavior. In order to increase the visibility of this effect, here we used the constant perturbations $d(k) = 0.1$, i.e., the maximum positive additive perturbation, at each time step.

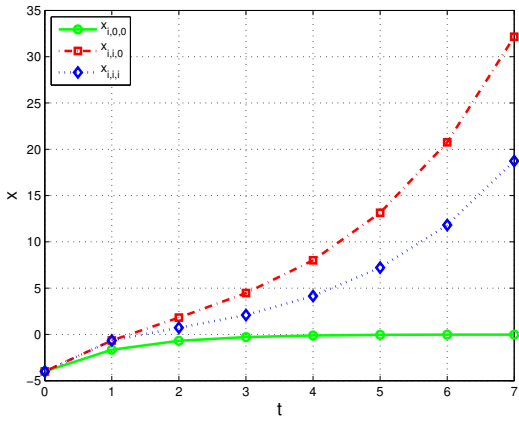


Fig. 3. State trajectories for the unstable system with $\alpha = 1.5$ with constraint $u \geq 0$ and maximum positive perturbation at each time step

TABLE II
COMPARISON OF CONTROL SCHEME PERFORMANCE

	$\alpha = 1.5$
$J_N^{\text{nom}}(x_0)$	42.0829
$J_N^{\text{pert}}(x_0)$	1763.9
$J_N^{\text{reopt}}(x_0)$	581.7244

VII. CONCLUSION AND OUTLOOK

In this work, we analyzed discrete time finite horizon optimal control problems and obtained estimates for the improvements brought about by re-optimizing at each iterate in the presence of disturbance on the system. The benefit of re-optimization is exhibited through relations involving moduli of continuity of objective functions and optimal value functions. These moduli are, in turn, determined by stability and controllability properties of the system under consideration. This work will be extended to the multistep feedback MPC setting from [10] aiming to conduct an analysis on the benefit of re-optimization for MPC schemes approximating infinite horizon optimal control problems.

REFERENCES

- [1] D. P. Bertsekas, Dynamic Programming and Optimal Control. Vol. 1 and 2. Athena Scientific, Belmont, MA, 1995.
- [2] C. Büskens, H. Maurer, Sensitivity analysis and real-time optimization of parametric nonlinear programming problems, in M. Grötschel, S. O. Krumke, J. Rambau, eds., Online Optimization of Large Scale Systems, Springer-Verlag, Berlin, 2001, 3–16.
- [3] M. Diehl, R. Findeisen and F. Allgöwer, A Stabilizing Real-time Implementation of Nonlinear Model Predictive Control, in L. Biegler, O. Ghattas, M. Heinkenschloss, D. Keyes and B. van Bloemen Waanders, eds., Real-Time and Online PDE-Constrained Optimization, SIAM, 2007, 25–52.
- [4] J. W. Eaton, and J. B. Rawlings, Feedback Control of Chemical Processes Using on-line Optimization Techniques, Comp. & Chem. Eng., 14 (1990), 469–479.
- [5] L. Grüne and J. Pannek, Nonlinear Model Predictive Control: Theory and Algorithms, Springer-Verlag, London, 2011.
- [6] B. Joseph and F. Wang Hanratty, Predictive Control of Quality in a Batch Manufacturing Process Using Artificial Neural Networks, Ind. Eng. Chem. Res. 32 (1993), 1951–1961.
- [7] T. Liu, F. Gao, Batch Process Control, Chapter 12 in T. Liu, F. Gao, Industrial Process Identification and Control Design, Springer-Verlag, London, 2012, 433–452.
- [8] H. Maurer and H. J. Pesch, Solution Differentiability for Parametric Nonlinear Control Problems with Control-State Constraints, SIAM Journal on Control and Optimization 32 (1991), 285–309.
- [9] Z. K. Nagy and R. D. Braatz, Robust nonlinear model predictive control of batch processes. AIChE J. 49 (2003), 1776–1786.
- [10] V. Palma, L. Grüne, Stability, performance and robustness of sensitivity-based multistep feedback NMPC, Extended Abstract in: Proceedings of the 20th International Symposium on Mathematical Theory of Networks and Systems — MTNS 2012, CD-ROM, Paper No. 68, 4 pages
- [11] H. J. Pesch, Numerical computation of neighboring optimum feedback control schemes in real-time, Applied Mathematics and Optimization 5 (1979), 231–252.
- [12] J. B. Rawlings and D. Q. Mayne, Model Predictive Control: Theory and Design. Nob Hill Publishing, Madison, 2009.
- [13] H.-R. Schwarz, R. Köckler, Numerische Mathematik, 5th ed., Teubner-Verlag, Wiesbaden, 2004
- [14] M. M. Thomas, J. L. Kardos, and B. Joseph, Shrinking Horizon Model Predictive Control Applied to Autoclave Curing of Composite Laminate Materials, Proc. of the American Control Conf., IEEE Press, Piscataway, NJ, 1994, 505–509.